Publications of the Astronomical Society of the Pacific
107: 104–119, 1995 February

The Physics of Massive OB Stars in Different Parent Galaxies. I. Ultraviolet and Optical Spectral Morphology in the Magellanic Clouds

NOLAN R. WALBORN
Space Telescope Science Institute,[1] 3700 San Martin Drive, Baltimore, Maryland 21218
Electronic mail: walborn@stsci.edu

DANIEL J. LENNON, STEPHAN M. HASER, AND ROLF-PETER KUDRITZKI
Institute for Astronomy and Astrophysics, Munich University, Scheinerstrasse 1, D-81679 Munich, Germany
Electronic mail: djl, haser, kudritzki@usm.uni-muenchen.de

STEPHEN A. VOELS
Astrophysics Data Facility, Code 631, Goddard Space Flight Center, Greenbelt, Maryland 20771
Electronic mail: voels@nssdca.gsfc.nasa.gov

Received 1994 September 19; accepted 1994 November 18

ABSTRACT. *HST*/FOS and ESO 3.6-m/CASPEC observations have been made of 18 stars ranging in spectral type from O3 through B0.5 Ia, half of them in each of the Large and Small Magellanic Clouds, in order to investigate massive stellar winds and evolution as a function of metallicity. The spectroscopic data are initially presented and described here in an atlas format. The relative weakness of the stellar-wind features in the SMC early O V spectra, due to their metal deficiency, is remarkable. Because of their unsaturated profiles, discrete absorption components can be detected in many of them, which is generally not possible in LMC and Galactic counterparts at such early types, or even in SMC giants and supergiants. On the other hand, an O3 III spectrum in the SMC has a weak C IV but strong N V wind profile, possibly indicating the presence of processed material. Wind terminal velocities are also given and intercompared between similar spectral types in the two galaxies. In general, the terminal velocities of the SMC stars are smaller, in qualitative agreement with the predictions of radiation-driven wind theory. Further analyses in progress will provide atmospheric and wind parameters for these stars, which will be relevant to evolutionary models and the interpretation of composite starburst spectra.

1. INTRODUCTION

The winds of OB stars significantly affect their evolution, and their mass-loss rates are expected to depend upon the metallicity since the winds are driven by momentum transfer from the radiation field via spectral-line absorption. Hence, it is essential to investigate mass loss as a function of metallicity in order to understand massive stellar evolution in different galaxies (e.g., Kudritzki et al. 1987a). This dependence must also be accounted for in the determination of extragalactic stellar distances from observations of the winds (Kudritzki et al. 1994), and to correctly interpret the integrated spectra of starbursts (Leitherer and Heckman 1995), which involve systems of differing metallicities.

The Magellanic Clouds offer the best opportunity to explore this problem, since they have different, lower metallicities than the Galaxy, and their individual OB members can be adequately observed with current instrumentation. Large ground-based telescopes in the Southern Hemisphere have been providing the required optical data for some time, but the *Hubble Space Telescope* provides the first UV capabilities reaching the necessary range and sample of spectral types for a systematic investigation. In observing programs led by R.-P.K., high-resolution optical spectroscopy has been obtained at the European Southern Observatory 3.6-m telescope to determine atmospheric parameters, and UV data for the same stars have been acquired with the *HST* Faint Object Spectrograph to investigate the winds. A sample of nine objects with approximately matched spectral types in each Cloud has been observed in this way. These observations include the first high-quality UV data for early-O main-sequence objects in the SMC, whose wind profiles will be shown to be more sensitive to the metal deficiency than those of the giants and supergiants analyzed previously, due to saturation effects in the latter. Both the optical and UV data for all 18 stars are presented in the form of a spectral atlas and their salient morphological characteristics are discussed in this paper. Subsequent publications will present the atmospheric and wind parameters derived from these data by detailed modeling.

2. OBSERVATIONS AND REDUCTIONS

2.1 Targets

Stellar and exposure data for the observed sample are presented in Table 1. Star numbers are from Sanduleak (Sk) (1970) in the LMC and from Azzopardi and Vigneau (AV) (1975, 1982) in the SMC, except for the members of NGC 346. Any revisions to prior spectral classifications are discussed in Sec. 3 below. The absolute visual magnitudes have been calculated with $(B-V)_0$ intrinsic colors of -0.32 for spectral types O3–O7, -0.31 for O9, -0.29 for O9.7, and -0.25 for B0.5; a ratio of total-to-selective extinction of 3.0;

[1]Operated by the Association of Universities for Research in Astronomy, Inc., under contract with the National Aeronautics and Space Administration.

TABLE 1
Target and Exposure Data

Star	Spectral Type	V	$B-V$	M_V	UV Exp [min] G130H	UV Exp [min] G190H	Galaxy	v_∞ [km s^{-1}]	v_r [km s^{-1}]
Sk−67°211	O3 III(f*)	12.28	−0.23	−6.6	31	13	LMC	3750	264
Sk−68°137	O3 III(f*)	13.26	−0.07	−6.1	95	40	LMC	3400	273
Sk−66°172	O3 III(f*)+OB	13.13	−0.12	−6.1	98	46	LMC	3250	303
NGC 346#3	O3 III(f*)	13.50	−0.23	−5.9	81	37	SMC	2900	161
Sk−67°166	O4 If+	12.27	−0.22	−6.6	33	12	LMC	1900	259
Sk−67°167	O4 Inf+	12.54	−0.19	−6.45	46	20	LMC	2150	290
AV 388	O4 V	14.12	−0.21	−5.3	178	87	SMC	2100	187
NGC 346#6	O4 V((f))	14.02	−0.24	−5.3	156	74	SMC	2250	200
NGC 346#4	O5-6 V	13.66	−0.23	−5.7	202	84	SMC	1550	157
AV 243	O6 V	13.87	−0.22	−5.5	233	89	SMC	2050	210
NGC 346#1	O4 III(n)(f)	12.57	−0.20	−6.9	47	20	SMC	2650	155
Sk−70°69	O5 V	13.96	−0.25:	−4.85	154	69	LMC	2600	283
Sk−66°100	O6 II(f)	13.26	−0.21	−5.7	88	42	LMC	2150	309
AV 238	O9 III	13.77	−0.22	−5.6	178	83	SMC	1200	240
AV 232	O7 Iaf+	12.36	−0.21	−7.1	36	16	SMC	1400	164
Sk−65°21	O9.7 Iab	12.02	−0.16	−7.0	47	25	LMC	1600	281
Sk−68°41	B0.5 Ia	12.01	−0.14	−6.9	58	28	LMC	1050	239
AV 488	B0.5 Iaw	11.90	−0.13	−7.6	53	23	SMC	1300	193

and distance moduli of 18.6 for the LMC and 19.1 for the SMC. The UV exposure times, stellar-wind terminal velocities determined from the UV line profiles, and heliocentric radial velocities measured from the optical data are also given in the table.

2.2 Ultraviolet

The UV observations were obtained with the *Hubble Space Telescope* (*HST*) and the Faint Object Spectrograph (FOS) between 1992 June 4 and 1993 October 27 under program IDs 2233/4110. The blue detector, in combination with the G130H and G190H gratings and the slit aperture (0.25×2.0 arcsec), was used to obtain spectrograms of each star in the wavelength regions 1140–1606 Å and 1573–2330 Å. The total exposure times for each star are given in Table 1; in a number of cases the exposures were done in multiple integrations during consecutive *HST* orbits. The signal-to-noise ratios of the resultant co-added spectrograms range from about 70 to 100 per pixel and the resolutions of these data are approximately 1.0 and 1.5 Å FWHM for the G130H and G190H gratings, respectively.

Two features in the pipeline-processed data were immediately noticed as anomalous: the presence of spikes due to the use of incorrect dead-diode reference files, and the nonsaturation of P-Cygni absorption troughs (and Lyα absorption). The first of these anomalies was easily removed by recalibrating the data in STSDAS using more appropriate calibration reference files and tables (Taylor and Keyes 1993), although an apparent emission feature at about 1500 Å in the spectrum of AV 388 is due to intermittent operation of a diode during an exposure. The second anomaly was caused by a combination of two effects: an incorrect model for the particle-induced background signal plus the presence of scattered (red) light on the detector (Rosa 1993a, b; Kinney 1993); for the G130H data these effects were corrected approximately following the algorithm of Rosa (1993b). It was found that even after this correction procedure a number of stars had suspiciously not-quite saturated P-Cygni troughs; however, this residual effect could be due to close companions contributing light through the aperture in some cases, as further discussed below. One final reduction problem should be mentioned, namely the flux calibration. As has been pointed out by, e.g., Bohlin et al. (1990), and Rosa and Benvenuti (1994), inaccuracies in the calibrations of absolute flux standards are evident when one compares model predictions with observations. These flaws are also evident in our data (Lennon et al. 1993), but no steps have been taken to correct them using the method based on white-dwarf models (Bohlin 1993) since we are interested here only in normalized spectrograms and major features therein. The normalization was done with splines. The geocoronal Lyα emission has been clipped at the continuum in a few cases in which it exceeded the latter, and a median filter of width 0.5 Å was applied. We have also merged the separate wavelength regions and restricted the displayed range to 1150–1750 Å, which contains the major features of interest.

2.3 Optical

The optical spectrograms were obtained with the European Southern Observatory (ESO) 3.6-m telescope and its Cassegrain echelle spectrograph (CASPEC) in four separate observing runs during 1984, 1985, 1986, and 1987. The detector was an RCA 512×320-pixel CCD (pixel size 30×30 microns), which was binned in the dispersion direction producing an effective 2-pixel resolution at Hγ of approximately 0.5 Å; the slit width was 2.0 arcsec. The 31.6 lines mm^{-1} echelle grating was used to obtain a useful wavelength coverage from about 4000 to 5000 Å. A typical exposure time

was 120 min for a star with $B=13.0$, and the S/N ratios of these data range between 30 and 70 per pixel.

The bluest orders of the echellograms are too closely packed to allow reliable background estimates. Additionally, the CCD used had a defective column (#48) which smeared part of its charge into a neighboring column (#49), resulting in the corruption of a number of orders shortward of Hδ. The more obvious manifestations of this fault have been excised from the final spectrograms, but in all cases the Hδ profile itself is also not reliable. The echelle orders were extracted in the MIDAS environment, but the correction for the blaze function was performed explicitly for each order using splines. Finally, for display and classification purposes, the data were rebinned to a resolution of 1 Å FWHM, they were median-filtered to remove remaining cosmic-ray events, and strong nebular emission lines were artificially suppressed.

3. CHARACTERISTICS OF THE SPECTRA

The UV and optical data are presented in Figs. 1–10, which are facing montages of both wavelength ranges for each of five spectral-type groupings. In general, the optical characteristics, which determine the spectral classifications, will be discussed first, followed by the UV wind properties.

3.1 O3 Giants (Figs. 1 and 2)

These spectra show the strong, narrow N IV λ4058 emission and N V λλ4604,4620 absorption lines characteristic of the type; Sk−67°211=HDE 269810 is the prototype of the class (Walborn 1982), for which a very large mass has been derived (Puls et al. 1994). Weak Si IV λλ4089,4116 emission is detected in the present observation. As expected, He I is not present in these spectra, except for Sk−66°172, which has a quite strong λ4471 absorption; this line is here assumed to arise in an OB companion to the O3 star, as denoted in the spectral classification, since it is inconsistent with the strong N IV and N V features. The O3 classification of this spectrum is newly determined by the present data. Sk−68°137 was so classified by Garmany and Walborn (1987), and a preliminary optical/UV analysis was given by Kudritzki et al. (1992). NGC 346 No. 3 was found in the largest H II region of the SMC by Walborn and Blades (1986) and Niemela et al. (1986); an atmospheric analysis was presented by Kudritzki et al. (1989).

The UV spectra of these stars all show the strong O V λ1371 wind profile which is a unique feature of O3 giants and supergiants (Walborn et al. 1985). The unsaturated resonance wind absorptions in Sk−66°172 may be further evidence of a companion. The most surprising result is the very weak C IV λλ1548,1551 wind profile in NGC 346 No. 3, which will be shown below to be a systematic property of SMC early-O main-sequence spectra, but in this case coexistent with a strong, saturated N V λλ1239,1243 profile. This configuration immediately suggests an enhanced N/C abundance ratio, likely due to CNO-cycled material in the wind of this star (Walborn and Panek 1985), although such an effect has not been seen before at this spectral type and the interpretation is not obviously supported by the strength of N IV λ1718 (although the latter feature is stronger than in the SMC early-O dwarfs). An alternative possibility is an anomalously high wind ionization, but that is not supported by the O V. Quantitative analysis will be required to interpret this remarkable spectrum; preliminary work by S.M.H. indicates that a very large N/C abundance ratio is in fact required to fit this spectrum. Perhaps all of these objects have enhanced N/C in their winds, but it is obvious only in the SMC star because the lower baseline metal abundance results in a desaturated C IV profile.

3.2 Two O4 If Stars in the LMC (Figs. 3 and 4)

The very close spectral, luminosity, and spatial relationships of these two stars were noted by Garmany and Walborn (1987), the only distinctions being the greater (presumably rotational) line broadening in Sk−67°167, and the fact that Sk−67°166=HDE 269698 had been discovered much earlier. The weak N IV (weaker than N III λλ4634–4640–4642) and Si IV emission and N V absorption are characteristic of the class with adequate resolution and S/N (Walborn 1971; Walborn and Fitzpatrick 1990), as are the small but definite He I/He II absorption ratios.

The close similarity of the two spectra extends to the UV, observed here with high quality for Sk−67°167 for the first time, with one surprising exception: the great relative strength of the C III λ1176 wind profile in Sk−67°167. This feature is also quite strong in ζ Puppis, O4 I(n)f (Snow and Morton 1976), which is likewise a rapid rotator. On the other hand, the C III feature appears quite weak in an *IUE* high-resolution observation of HD 190429A, O4 If+ (I. Howarth, private communication). The spectra of ζ Pup, HD 190429A, and HDE 269698 are very similar in the 1200–1900 Å range (Walborn et al. 1985). Again, quantitative analysis will be required to explain the origin of this discrepancy.

3.3 Early-O Dwarfs in the SMC (Figs. 5 and 6)

The great strength of the He II λ4686 absorption determines luminosity class V for all of these spectra, including AV 243=Sk 84 (Sanduleak 1968) which had been classified O6 III by Garmany and Conti (1987). NGC 346 No. 6 is the relatively bright star just west of Nos. 3 and 4 in Fig. 1 of Walborn and Blades (1986), also No. 32 of Niemela et al. (1986) and No. 324 of Massey et al. (1989).

The extreme weakness of the UV C IV, N IV, and N V wind profiles compared to Galactic and LMC counterparts at these early spectral types (cf. Walborn et al. 1985 and the next section) is remarkable and one of the most important results of this investigation. Effects of the SMC metal deficiency on the stellar winds of member giants and supergiants have been described previously (e.g., Bruhweiler et al. 1982; Fitzpatrick 1984; Garmany and Conti 1985; Garmany and Fitzpatrick 1988), but they are far more pronounced in these main-sequence spectra, which have not been observed before with the present quality. Pending quantitative analysis, this circumstance may be preliminarily ascribed to saturation in these very sensitive transitions in the denser giant and supergiant winds, even at the SMC metallicity. The unsaturated C IV and N V wind profiles in the SMC main-sequence objects also permit the detection and study of discrete absorp-

tion components (Howarth and Prinja 1989) at these early spectral types, which is generally prevented by saturation of the broad absorption in Galactic and LMC counterparts.

3.4 O-Type Giants (Figs. 7 and 8)

NGC 346 No. 1 is the brightest object in the compact ionizing cluster of the largest SMC H II region; its very early spectral type was found by Walborn (1978). Heydari-Malayeri and Hutsemékers (1991) showed that it is a composite object, but it is likely that the brightest component dominates the present data due to the relatively large separations and the small apertures used. Weak N III and N IV emissions are detected as reported by Walborn (1978), and He II λ4686 has a P-Cyg profile, which is unusual (see also Kudritzki et al. 1989). The LMC main-sequence star Sk −70°69 has been included in these figures as a result of the reclassification of AV 243 mentioned in the previous section. Sk−66°100 had also been classified O6 III by Conti et al. (1986), but the very weak He II λ4686 absorption and strong N III emission lead to the present classification. Weak Si IV and N III absorption lines are also detected, as is possible weak C III λ4650 emission. The present optical spectrogram of AV 238 is in agreement with the prior classification by Garmany and Conti (1987).

The UV wind profiles in NGC 346 No. 1 are nearly normal despite the SMC metal deficiency, which may be understood in terms of saturation effects in the relatively dense wind of this early-O giant star. If this spectrum were significantly contaminated by flux from the companions, such that the intrinsic wind absorption is actually black, then a terminal velocity as low as 2250 km s^{-1} could be derived due to the greater contribution from turbulence. Although the wind profile shapes in the LMC object Sk−70°69 are reasonably normal for the spectral type, their highly unsaturated absorptions are a puzzle, if not of instrumental origin. It may be relevant that also the absolute visual magnitude derived for this star (Table 1) is abnormally faint for its spectral type (Walborn 1973). The wind features of the LMC star Sk −66°100 are normal for its spectral type, including the incipient Si IV λλ1394,1403 profile (Walborn and Panek 1984; Walborn et al. 1985; Pauldrach et al. 1990); a preliminary analysis of this spectrum was given by Kudritzki (et al. 1992). The wind of AV 238 is somewhat weak relative to Galactic counterparts (Walborn et al. 1985), consistent with the SMC metal deficiency and the relatively low density in a late-O giant wind.

3.5 OB Supergiants (Figs. 9 and 10)

AV 232=Sk 80 is the well-known Of object located within the eastern periphery of NGC 346, and so far the only normal representative of that spectroscopic category in the SMC. As noted by Walborn (1977), the essentially normal, strong N III features in its spectrum despite the SMC metal deficiency may indicate the presence of processed material in its atmosphere. Weak C III λ4650 emission is also detected here, as are the unidentified features at λλ4485,4503. The weakness of Si IV λ4089 is probably due to a combination of metal deficiency and competition between absorption and emission in this line; note the presence of λ4116 in emission (denoted by + in the spectral type). Optical atmospheric analyses of the other three stars in these figures have been performed by Kudritzki et al. (1987b) and Lennon et al. (1991); note AV 488=Sk 159. Sk−65°21 has been reclassified here as O9.7 Iab on the basis of He II λ4541≈Si III λ4552 (spectral type) and the strengths of Si IV λλ4089,4116 and He II λ4686 (luminosity class)—see also Fitzpatrick (1988) and Walborn and Fitzpatrick (1990). The unidentified emission lines at λλ4485,4503 are also present here. This spectrum provides a nice example of CNO morphological normalcy for its type, while Kudritzki et al. (1987b) found CNO-cycled abundances in its atmosphere, in agreement with the hypothesis of Walborn (1976) regarding the OBN/OBC anomalies. The same remarks apply to Sk−68°41; see also Lennon et al. (1991). The Si III λ4552/Si IV λ4089 ratio in Sk−68°41 places it at the cool end of the B0.5 class, although not quite at B0.7; in particular, it is likely somewhat cooler than AV 488 despite the same classifications. The "w" in the spectral type of AV 488 denotes the weakness of the metallic lines, as discussed by Walborn (1977,1983).

In keeping with their supergiant nature, all of these spectra display fully developed Si IV λλ1394,1403 wind profiles (Walborn and Panek 1984; Walborn et al. 1985; Pauldrach et al. 1990), as well as C III λ1176 (Snow and Morton 1976). However, the Si IV in AV 232 reveals the effects of a low terminal velocity relative to its Galactic counterparts, in the recovery of the emission from the shortward component of the doublet. Also, the wind features from the subordinate transitions of He II λ1640 and N IV λ1718 are anomalously strong for the spectral type, more similar to those in Galactic and LMC early-Of spectra; modeling may explain this discrepancy. The wind profiles of the other stars are reasonably normal for their spectral types (Walborn and Nichols-Bohlin 1987), even in AV 488 (see also Fitzpatrick 1984), which may be understood as a saturation effect in this very luminous object.

4. THE TERMINAL VELOCITIES

Terminal velocities determined from the UV wind profiles of all stars in the present sample are listed in Table 1, and they are plotted in Fig. 11 as a function of spectral type, with the different galaxies and luminosity classes distinguished. For comparison, mean values of measurements in Galactic counterparts from the *IUE* samples of Howarth and Prinja (1989) and Prinja et al. (1990) are also plotted; for consistency with the present results, they have been redetermined by S.M.H. with an SEI code (Haser et al. 1994). Altogether, 94 Galactic stars of luminosity classes V, IV and I, Ia, Iab are involved in the plotted means.

In general, Fig. 11 shows the expected trends for radiatively driven winds as functions of temperature, luminosity, and metallicity: lower terminal velocities at lower temperatures and metallicities due to the reduced driving force, and at higher luminosities due to the greater radii and densities. Some interesting systematic and individual deviations from the trends deserve comment, however. (i) The LMC O3 III stars have terminal velocities similar to or higher than the

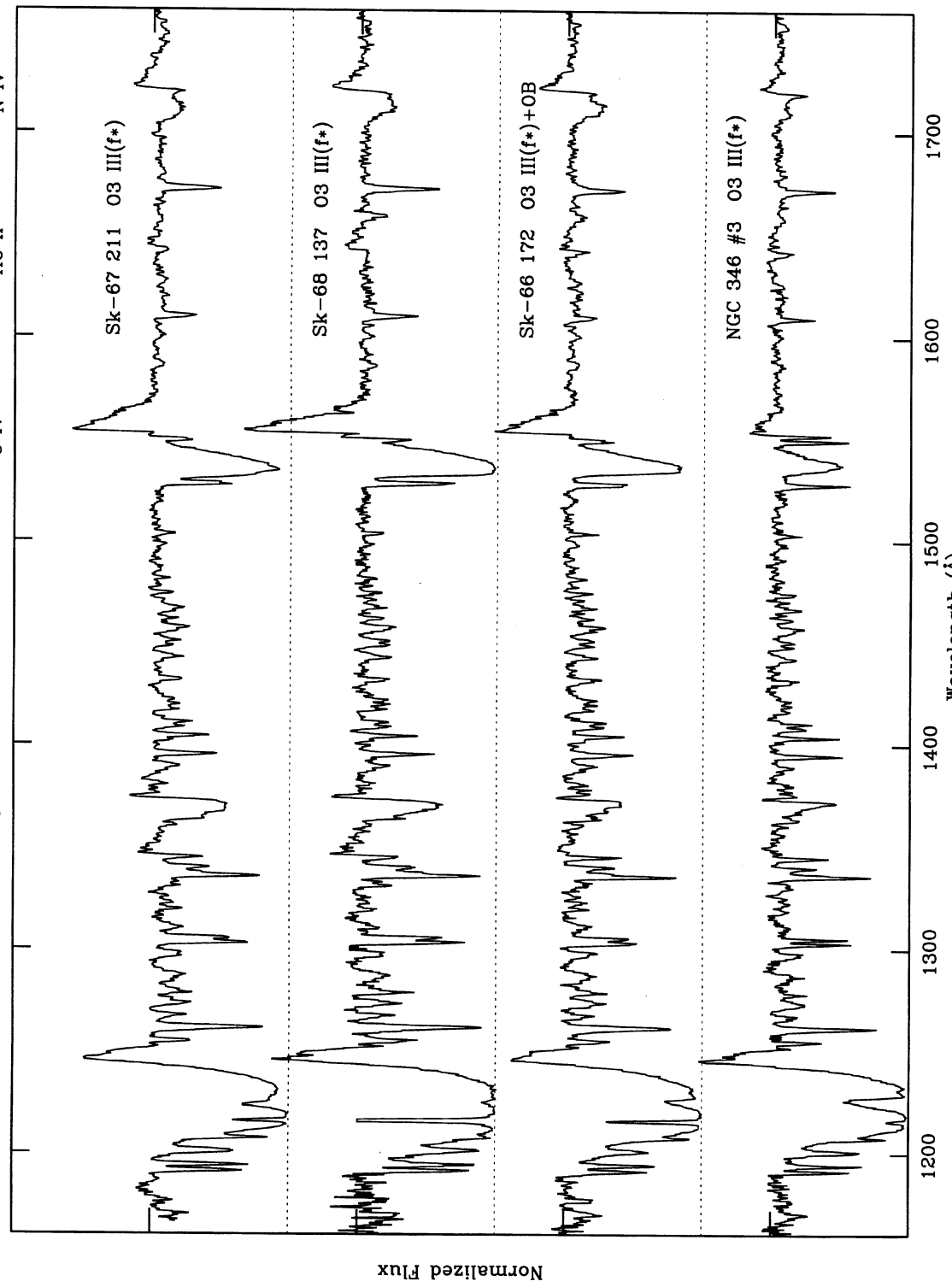

FIG. 1—Rectified *HST*/FOS ultraviolet spectrograms of three LMC O3 giants and one in the SMC. In this and subsequent UV figures, the ordinate ticks are separated by 1.5 continuum flux units; the zero levels are given by the lower border and the dashed lines. The geocoronal Lyα emission has been clipped at the continuum when it exceeded the latter. The stellar-wind features identified at the top are N V $\lambda\lambda$1239, 1243; O V λ1371; C IV $\lambda\lambda$1548, 1551; He II λ1640; and N IV λ1718. Note the well-marked O V wind profiles, characteristic of O3 giant spectra, in all of the stars, and the remarkable ratio of the N V-to-C IV wind profiles in the SMC star NGC 346 No. 3.

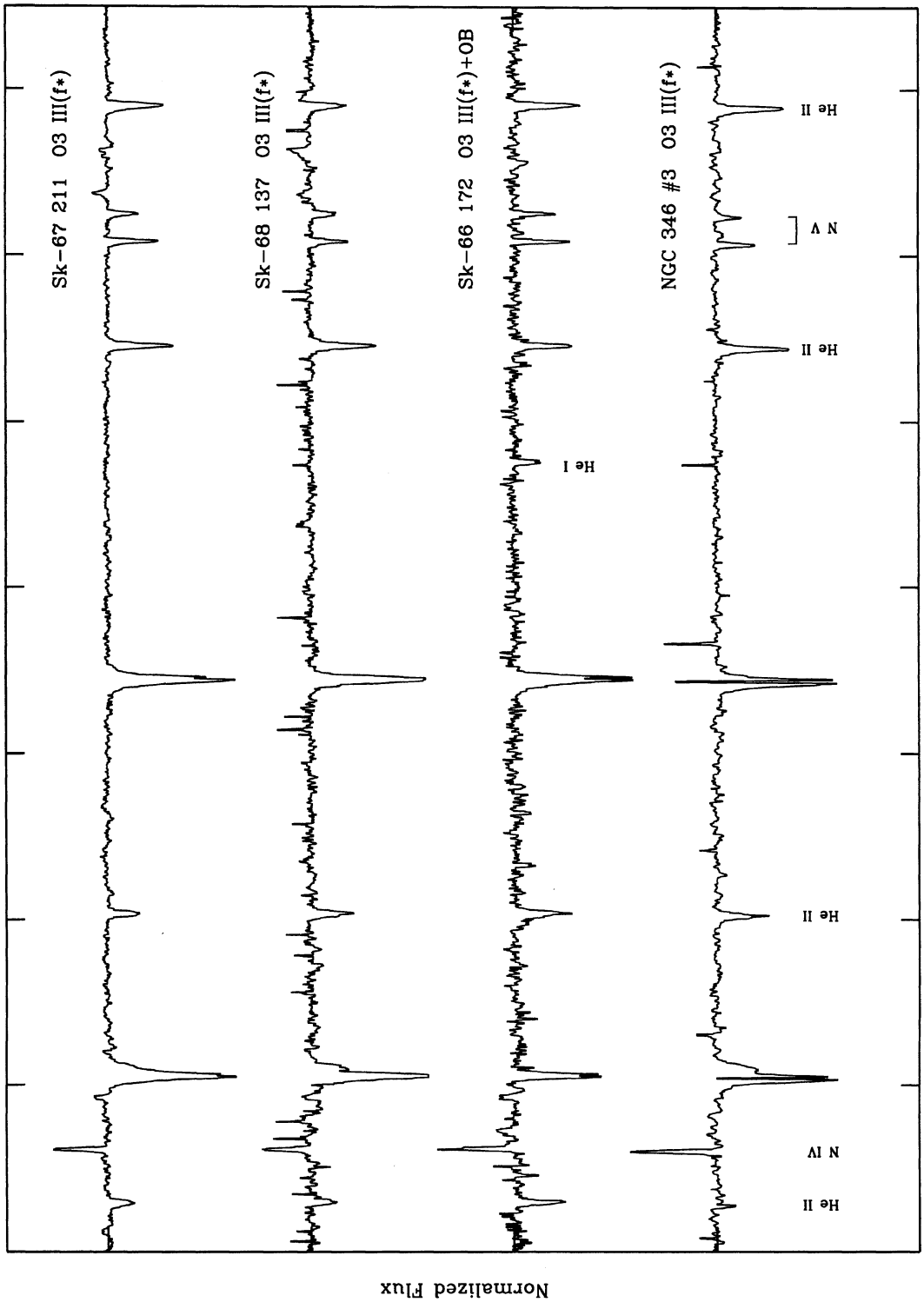

FIG. 2—Rectified ESO/CASPEC blue-violet spectrograms of the same stars shown in Fig. 1. In this and subsequent optical figures, the ordinate ticks are separated by 0.5 continuum flux units. Strong cosmic-ray and nebular-emission spikes have been truncated. The spectral lines identified in NGC 346 No. 3 are, from left to right by ion, He II λλ4026, 4200, 4541, 4686; N IV λ4058 emission; and N V λλ4604, 4620. In addition, the anomalous He I λ4471 feature in Sk−66°172 is identified, and He I likely contributes to the strong λ4026 feature as well; the He I is assumed to arise from a companion star, as denoted in the spectral type, in view of its inconsistency with the strong N IV and N V features characteristic of O3 giant spectra. The Balmer series members Hδ λ4101 and Hγ λ4340 are not explicitly identified in the figures; their emission cores in some spectra are nebular.

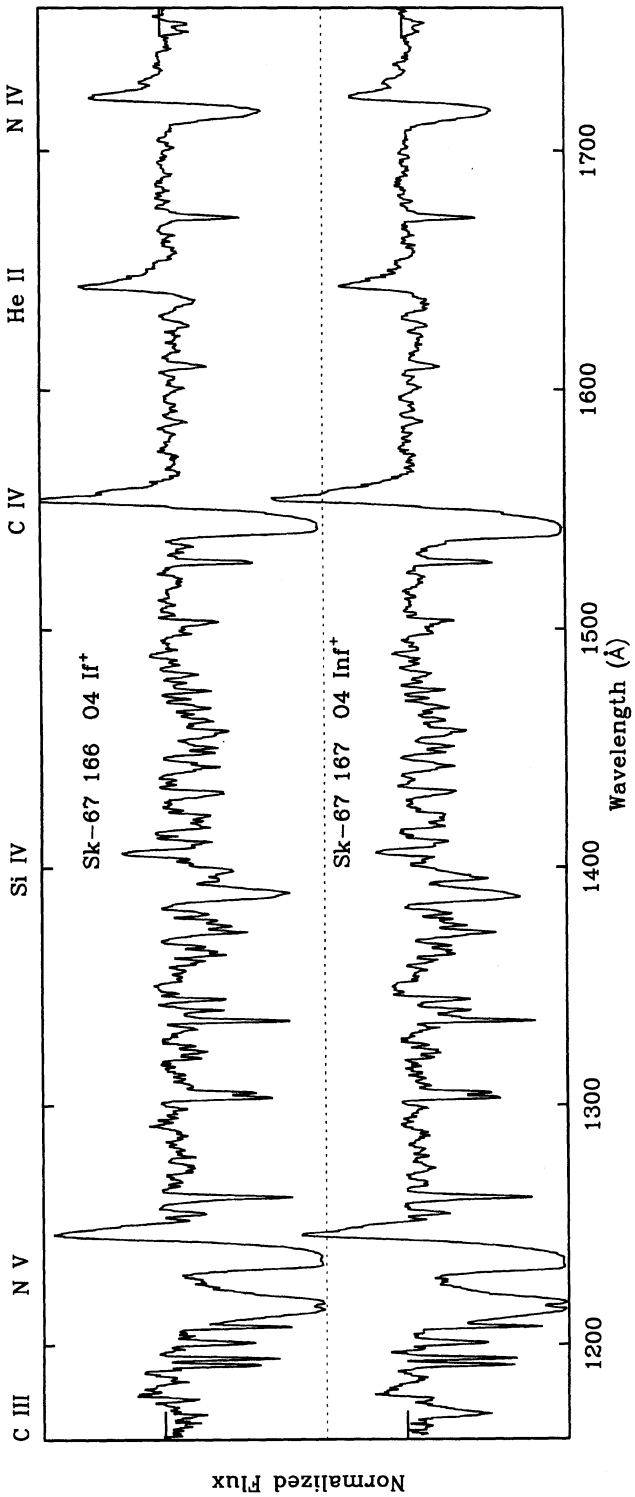

FIG. 3—UV spectrograms of two closely related O4 supergiants in the LMC. The stellar-wind features identified at the top are as in Fig. 1, with the addition of C III λ1176 and Si IV λλ1394, 1403. Note the detailed similarity of the two spectra, except for the much stronger C III wind profile in Sk−67°167; the latter may have stronger O IV λλ1339, 1343 wind features as well.

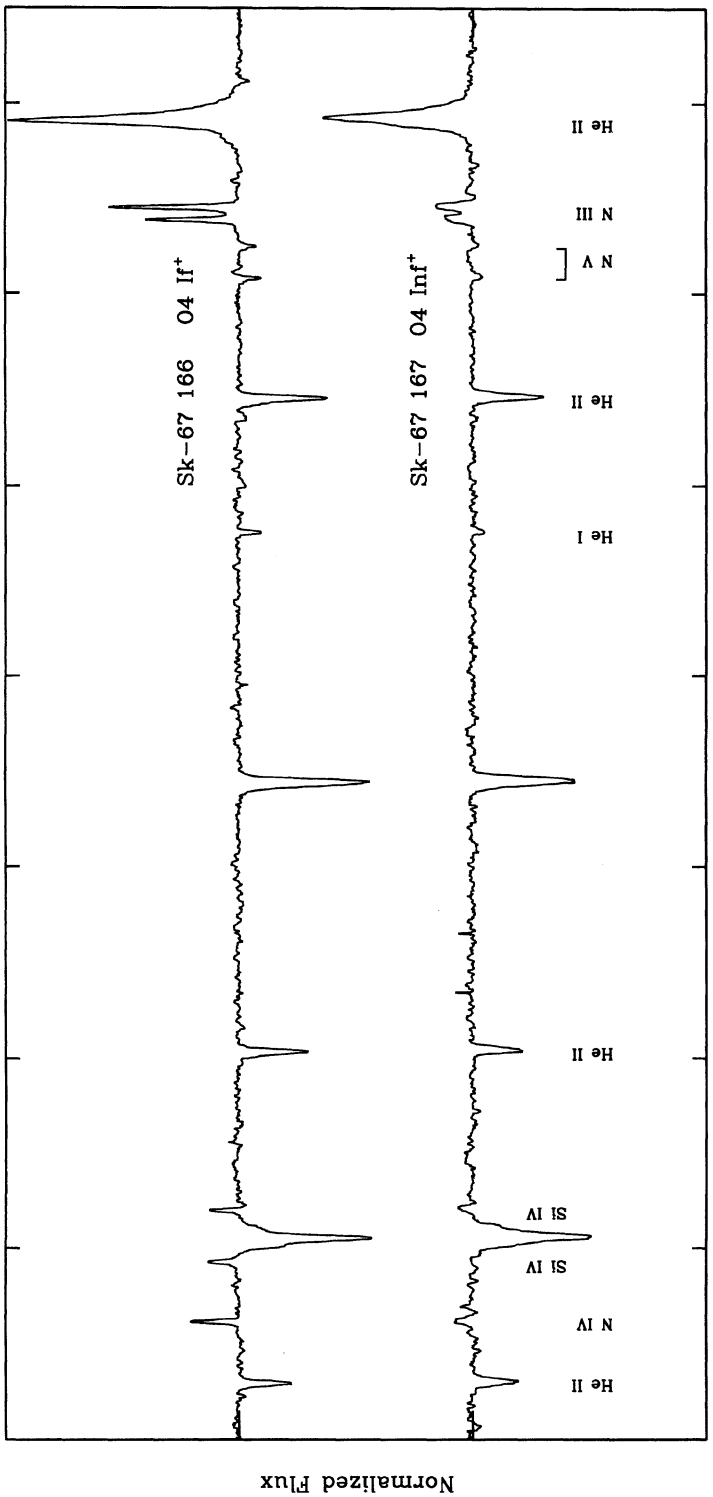

FIG. 4—Optical spectrograms of the same stars as in Fig. 3. The absorption lines identified in Sk−67°167 are He II λλ4026, 4200, 4541; He I λ4471; and N V λλ4604, 4620. The emission lines are N IV λ4058; Si IV λλ4089, 4116; N III λλ4634, 4640–42; and He II λ4686. All features are consistent with a smooth, systematic decline in ionization with respect to the O3 spectra in Fig. 2. The two O4 spectra are very similar to each other, except for the greater (rotational) line broadening in Sk−67°167, which affects both absorption and emission features comparably.

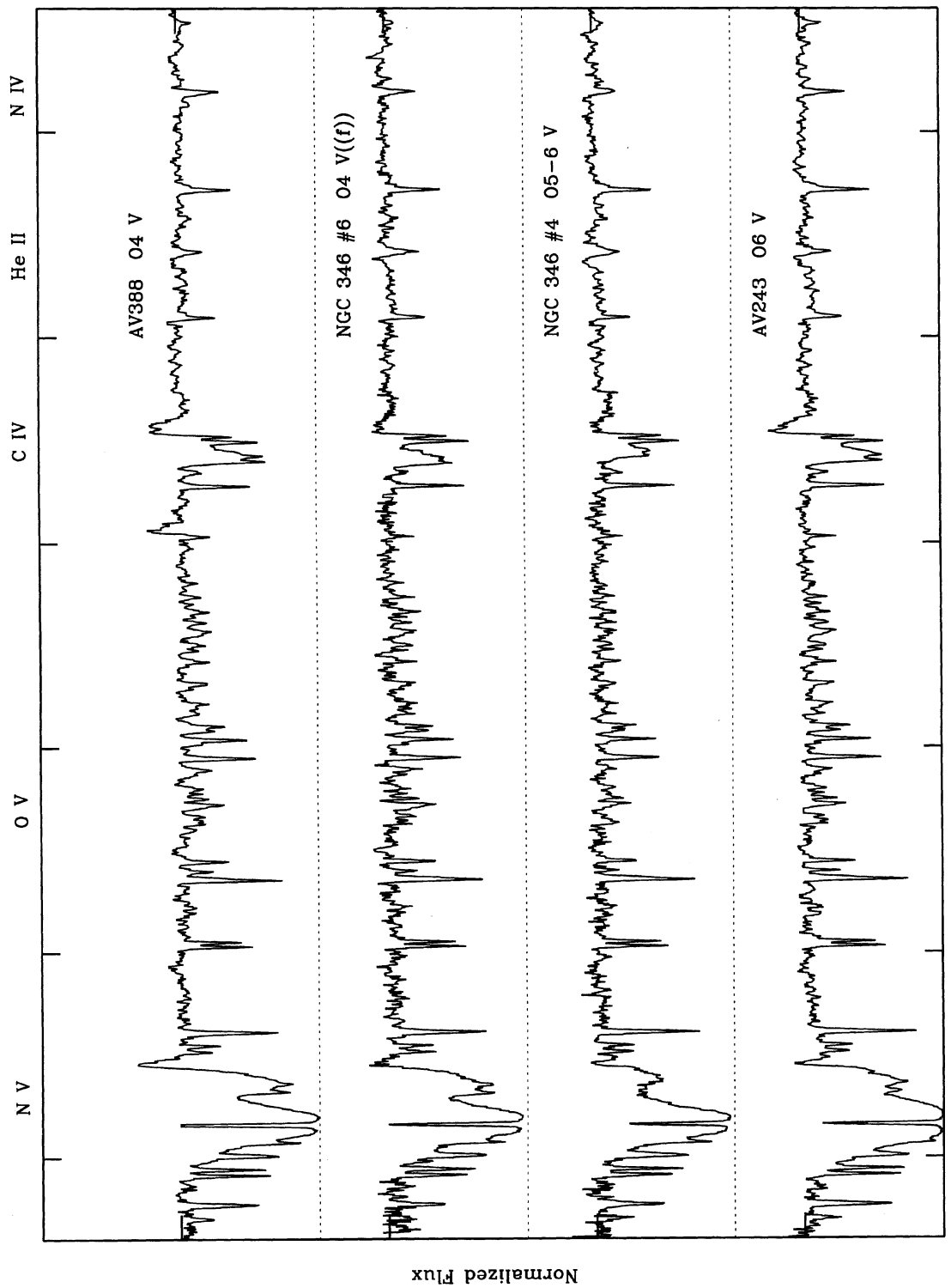

FIG. 5—UV spectrograms of four early-O dwarfs in the SMC. The apparent emission feature near 1500 Å in AV 388 is spurious (Sec. 2.2). The features identified at the top are as in Fig. 1. The stellar-wind profiles are extremely weak for the spectral types, due to the SMC metal deficiency. Shortward-displaced narrow absorption components are visible in most of the N V and C IV profiles. (The sharp, low-velocity C IV absorption doublets are interstellar.)

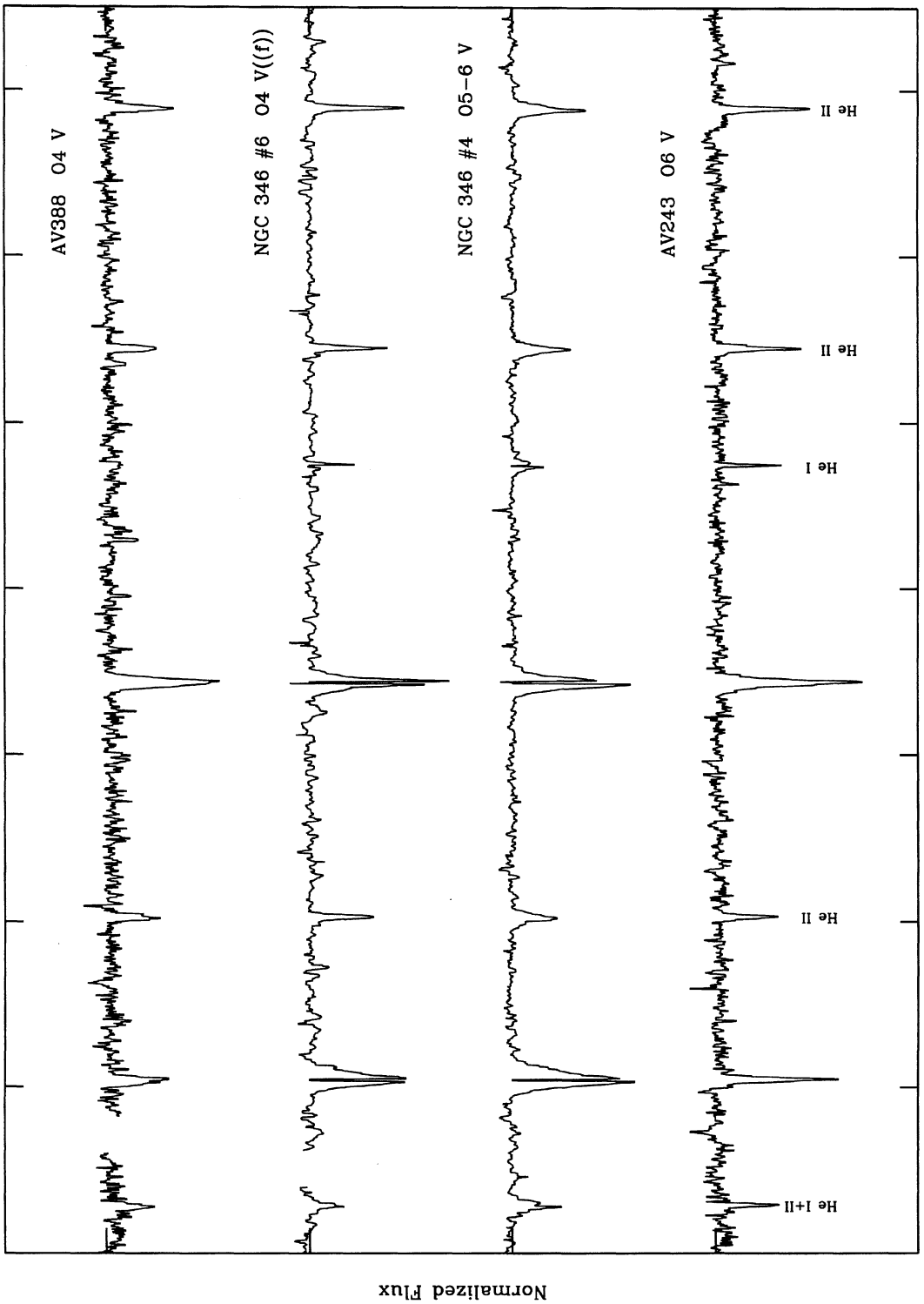

FIG. 6—Optical spectrograms of the stars in Fig. 5. Segments between 4000 and 4100 Å affected by a CCD defect have been omitted in AV 388 and NGC 346 No. 6 (Sec. 2.3). The spectral lines identified in AV 243 are He I+II λλ4200, 4541, 4686; and He I λ4471. The Balmer and He I lines are affected by sharp, nebular emission features in the NGC 346 stars.

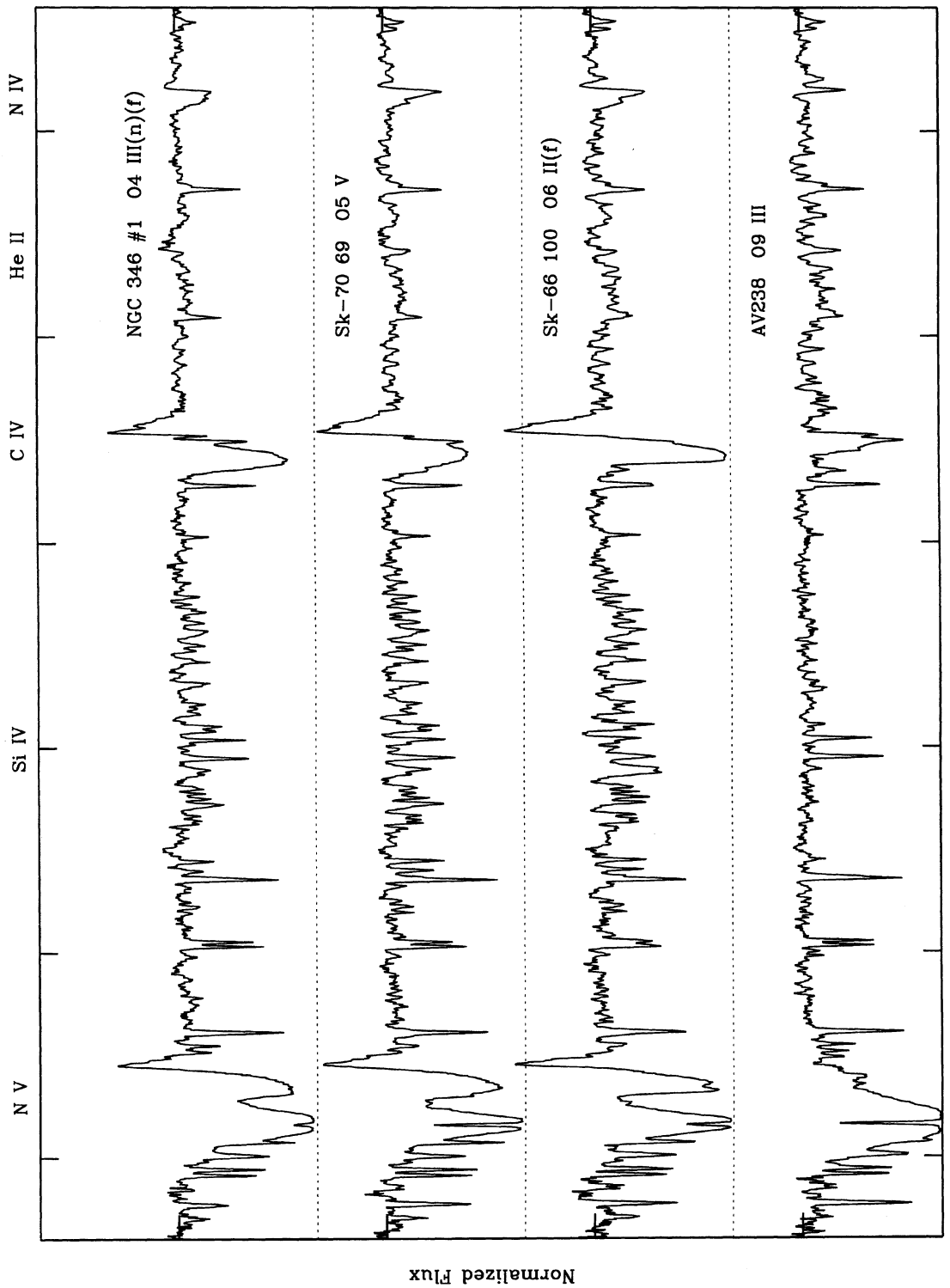

FIG. 7—UV spectrograms of two O-type giants in the SMC together with a dwarf and a bright giant in the LMC. The features identified at the top are as in Figs. 1 and 3. The somewhat diverse wind properties of these stars are discussed in Sec. 3.4.

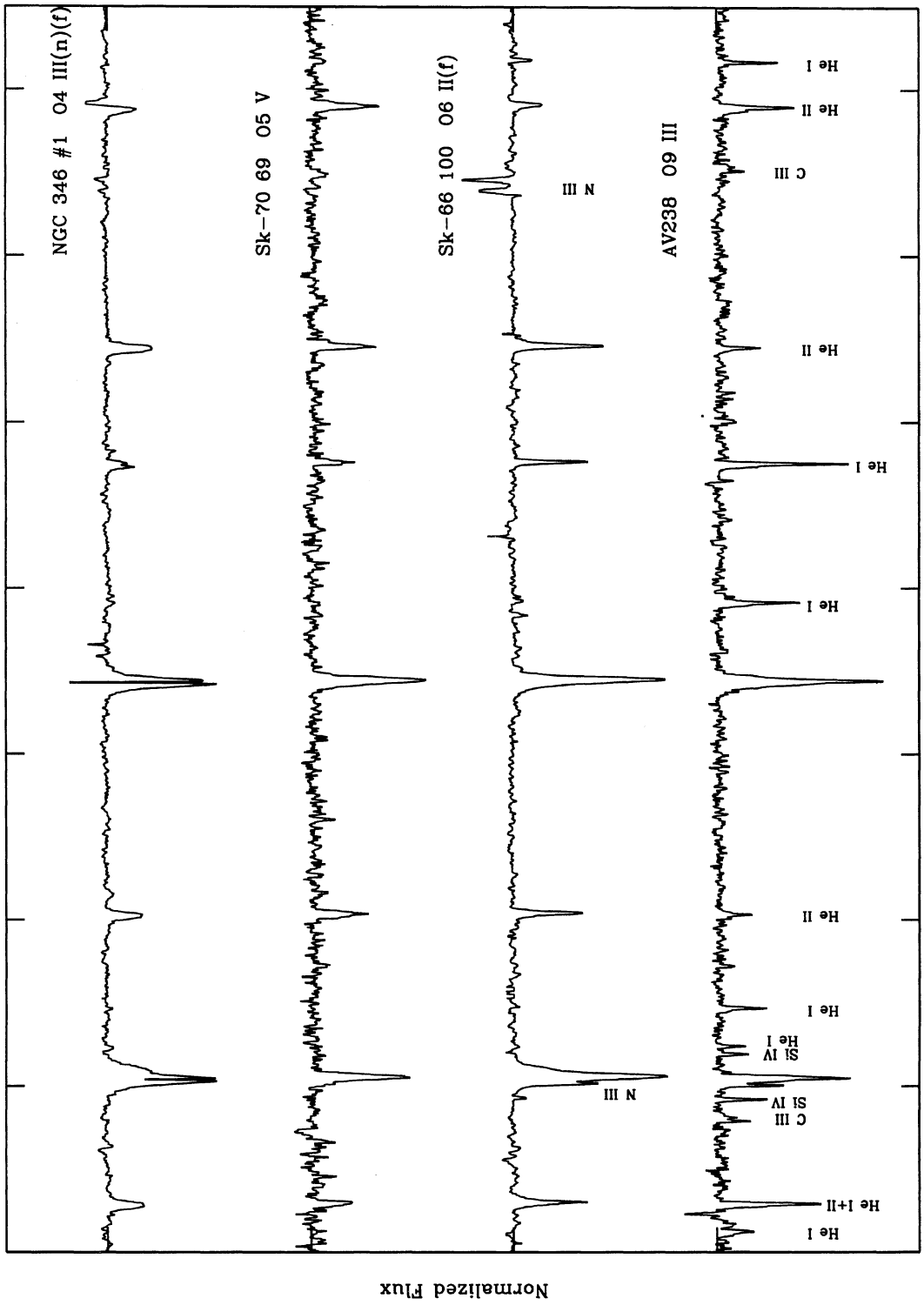

FIG. 8—Optical spectrograms of the stars in Fig. 7. The spectral lines identified in AV 238 are, from left to right by ion, He I λλ4009, (+II) 4026, 4121, 4144, 4387, 4471, 4713; He II λλ4200, 4541, 4686; C III λλ4070, 4650 blends; and Si IV λλ4089, 4116. In addition, N III λ4097 absorption and λλ4634, 4640–42 emissions are distinguished in Sk−66°100; the strengths of those emission features together with the greatly weakened (filled in by emission) He II λ4686 absorption lead to the luminosity class II. Note the unusual P-Cyg profile at λ4686 in NGC 346 No. 1; the sharp Balmer and He I emission features in this spectrum are nebular.

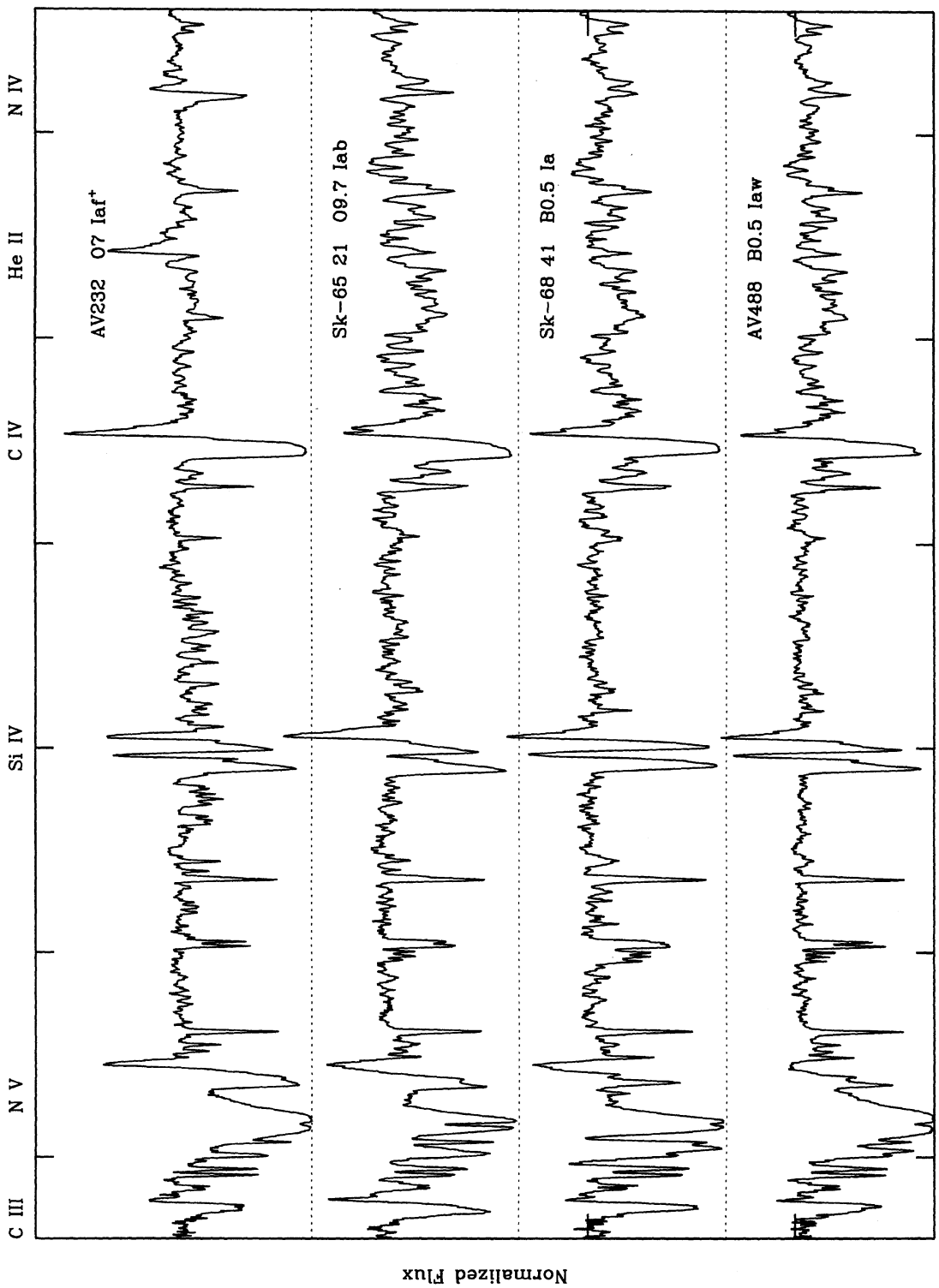

FIG. 9—UV spectrograms of four OB supergiants, two each in the LMC and SMC. The features identified at the top are as in Figs. 1 and 3. All of these spectra display fully developed Si IV wind profiles, as expected for their spectral types. The wind features from the subordinate He II and N IV transitions in AV 232 are anomalously strong for its spectral type.

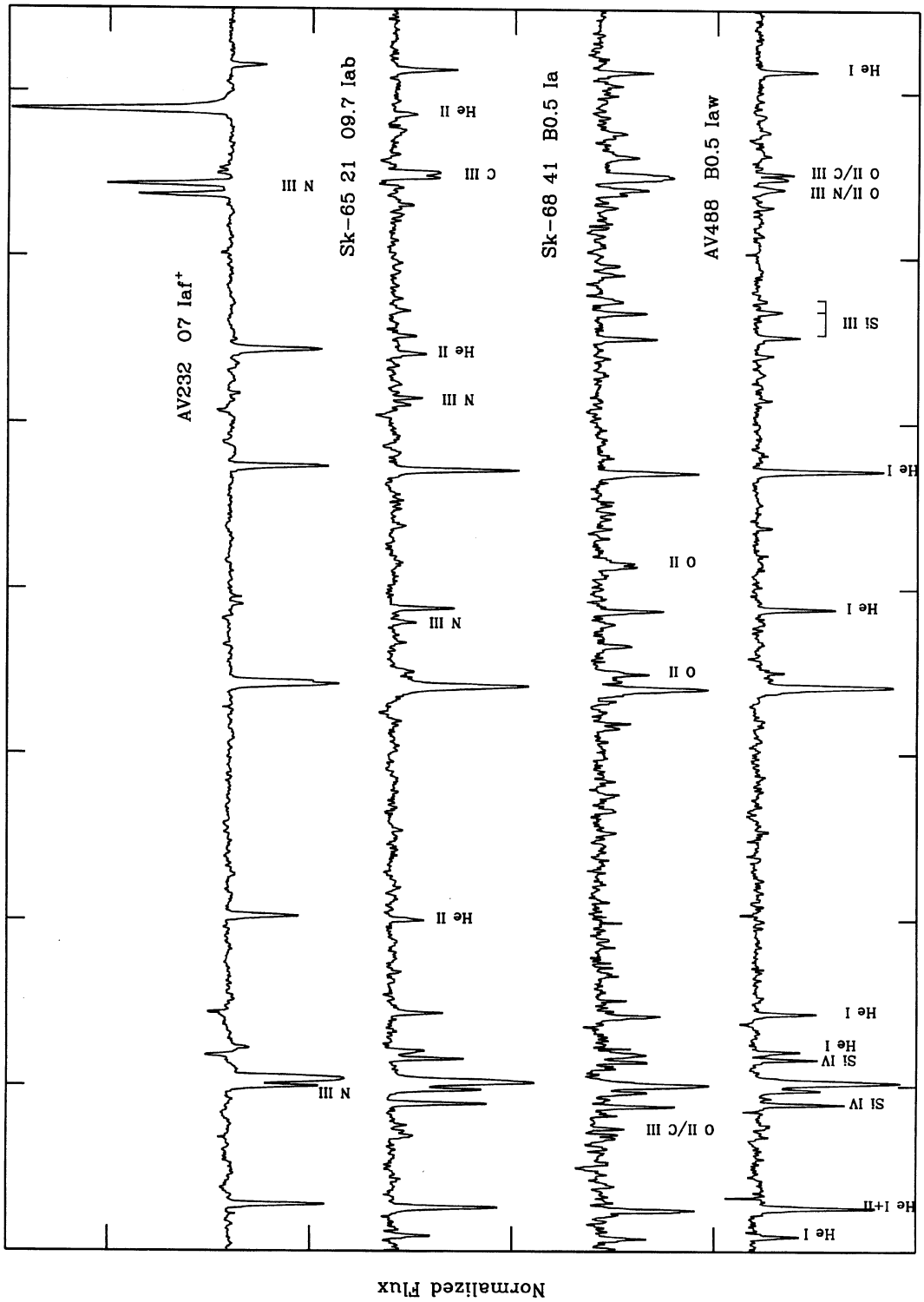

FIG. 10—Optical spectrograms of the same stars as in Fig. 9. The following spectral features are identified. In AV 488: He I λλ4009, (+II) 4026, 4121, 4144, 4387, 4471, 4713; Si IV λλ4089, 4116; Si III λλ4552, 4568, 4575; and O II/N III λ4640, O II/C III λ4650 blends. In Sk−68°41: O II/C III λ4070 and O II λλ4350, 4415–17 blends. In Sk−65°21: He II λλ4200, 4541, 4686; N III λλ4379, 4511–15; and C III λ4650 blend. In AV 232: N III λ4097 absorption and λλ4634, 4640–42 emissions. Note the comparable intensities of He II λ4541 and Si III λ4552 in Sk−65°21, leading to the O9.7 type. AV 488 may be somewhat hotter than Sk−68°41 on the basis of the Si III λ4552/Si IV λ4089 ratio; the metal lines are extremely weak in this very luminous SMC supergiant.

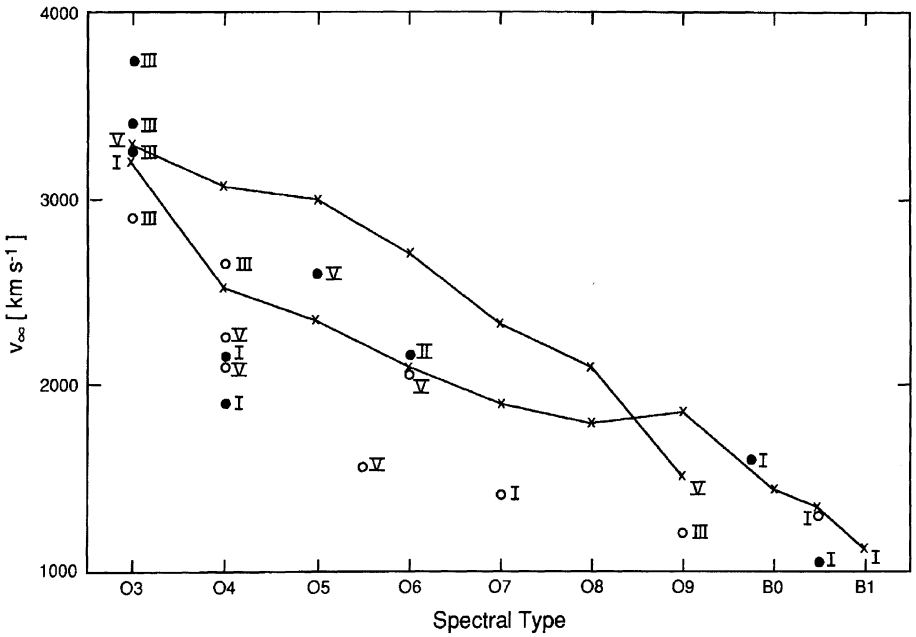

FIG. 11—Stellar-wind terminal velocities as a function of spectral type among the present LMC/SMC sample and Galactic counterparts. The different galaxies are distinguished by the following symbols: ×, the Galaxy, ●, LMC; ○, SMC, while the Galactic mean values for main-sequence and supergiant luminosity classes are connected by separate lines. The luminosity class corresponding to each point or line is specified in the figure. See Sec. 4 for discussion.

Galactic O3 V's despite lower metallicity and higher luminosity, indicating significantly greater temperatures and/or masses for the LMC objects. (ii) A possible reason for an overestimated terminal velocity in the SMC O4 III star NGC 346 No. 1 was noted in Sec. 3.4 above. (iii) The Galactic relations for dwarfs and supergiants cross over between spectral types O8 and O9, probably because the former lose their driving force more precipitously as the temperatures decline. (iv) Finally, it appears that the metallicity effects become relatively unimportant among the B supergiants, which may explain some previous discrepant conclusions regarding such effects as due to the particular types of stars under consideration. The relative discrepancy for the two B0.5 Ia stars may be related to the small spectral-type (temperature) difference mentioned in Sec. 3.5.

5. SUMMARY

A morphological review of high-quality, correlative UV (*HST*/FOS) and optical (ESO/CASPEC) spectroscopy of a complementary sample of OB stars in the two Magellanic Clouds has revealed a rich array of systematic and individual phenomena for quantitative analysis. The metallicity variable between the Clouds themselves and with respect to the Galaxy provides the likely cause and the basis for interpretation of many of them. Further analysis of these effects will contribute to improved understanding of massive stellar winds, evolution, and more distant composite systems. Perhaps the most important results are the strikingly deficient wind profiles seen in the SMC early-O dwarfs, which diagnose the systemic metal deficiency more clearly than previous observations; and the unexpected evidence for a very large N/C abundance ratio in the wind of the SMC O3 III star NGC 346 No. 3. The very large wind terminal velocities of the LMC O3 III objects likely have significant implications for their physical parameters; one of them, Sk−67°211=HDE 269810, may be the most massive star currently known (Puls et al. 1994). The further analysis of these and other intriguing phenomena described above will be presented in subsequent publications.

This paper is partially based on observations made with the NASA/ESA *Hubble Space Telescope*, obtained at the Space Telescope Science Institute, which is operated by the Association of Universities for Research in Astronomy, Inc., under NASA Contract No. NAS5-26555. Support for this work was provided by NASA through Grant No. GO-2233.02-87A from the STScI. The paper is also partially based on observations obtained at the European Southern Observatory, La Silla, Chile. S.M.H. was supported by DFG Grant No. Pa477/1-1 and D.J.L. by BMFT Grant No. 010R90080.

REFERENCES

Azzopardi, M., and Vigneau, J. 1975, A&AS, 22, 285
Azzopardi, M., and Vigneau, J. 1982, A&AS, 50, 291
Bohlin, R. C. 1993, in Calibrating Hubble Space Telescope, ed. J. C. Blades and S. J. Osmer (Baltimore, STScI), p. 234
Bohlin, R. C., Harris, A. W., Holm, A. V., and Gry, C. 1990, ApJS, 73, 413
Bruhweiler, F. C., Parsons, S. B., and Wray, J. D. 1982, ApJ, 256, L49
Conti, P. S., Garmany, C. D., and Massey, P. 1986, AJ, 92, 48
Fitzpatrick, E. L. 1984, ApJ, 282, 436
Fitzpatrick, E. L. 1988, ApJ, 335, 703
Garmany, C. D., and Conti, P. S. 1985, ApJ, 293, 407

Garmany, C. D., and Conti, P. S. 1987, AJ, 93, 1070
Garmany, C. D., and Fitzpatrick, E. L. 1988, ApJ, 332, 711
Garmany, C. D., and Walborn, N. R. 1987, PASP, 99, 240
Haser, S. M., Puls, J., and Kudritzki, R.-P. 1994, in Evolution of Massive Stars, ed. D. Vanbeveren, W. van Rensbergen, and C. de Loore (Dordrecht, Kluwer), p. 187
Heydari-Malayeri, M., and Hutsemékers, D. 1991, A&A, 243, 401
Howarth, I. D., and Prinja, R. K. 1989, ApJS, 69, 527
Kinney, A. L. 1993, in Calibrating Hubble Space Telescope, ed. J. C. Blades and S. J. Osmer (Baltimore, STScI), p. 184
Kudritzki, R.-P., Lennon, D. J., and Puls, J. 1994, in Science with the VLT, ed. J. R. Walsh (Berlin, Springer) (in press)
Kudritzki, R.-P., Pauldrach, A., and Puls, J. 1987a, A&A, 173, 293
Kudritzki, R.-P., et al. 1987b, in ESO Workshop on the SN 1987A, ed. I. J. Danziger (Garching, ESO), p. 39
Kudritzki, R.-P., et al. 1989, A&A, 226, 235
Kudritzki, R.-P., et al. 1992, in Science with the Hubble Space Telescope, ed. P. Benvenuti and E. Schreier (Garching, ESO), p. 279
Leitherer, C., and Heckman, T. M. 1995, ApJS, 96, 9
Lennon, D. J., et al. 1991, A&A, 252, 498
Lennon, D. J., Kudritzki, R.-P., Pauldrach, A. W. A., Gabler, R., and Haser, S. M. 1993, in Calibrating Hubble Space Telescope, ed. J. C. Blades and S. J. Osmer (Baltimore, STScI), p. 423
Massey, P., Parker, J. W., and Garmany, C. D. 1989, AJ, 98, 1305
Niemela, V. S., Marraco, H. G., and Cabanne, M. L. 1986, PASP, 98, 1133
Pauldrach, A. W. A., Kudritzki, R.-P., Puls, J., and Butler, K. 1990, A&A, 228, 125
Prinja, R. K., Barlow, M. J., and Howarth, I. D. 1990, ApJ, 361, 607
Puls, J., et al. 1994, A&A (to be submitted)
Rosa, M. R. 1993a, ST-ECF Newslett., No. 20, p. 16
Rosa, M. R. 1993b, in Calibrating Hubble Space Telescope, ed. J. C. Blades and S. J. Osmer (Baltimore, STScI), p. 190
Rosa, M. R., and Benvenuti, P. 1994, A&A (in press)
Sanduleak, N. 1968, AJ, 73, 246
Sanduleak, N. 1970, Cerro Tololo Inter-American Obs. Contr., No. 89
Snow, T. P., Jr., and Morton, D. C. 1976, ApJS, 32, 429
Taylor, C. J., and Keyes, C. D. 1993, in Calibrating Hubble Space Telescope, ed. J. C. Blades and S. J. Osmer (Baltimore, STScI), p. 174
Walborn, N. R. 1971, ApJ, 167, L31
Walborn, N. R. 1973, AJ, 78, 1067
Walborn, N. R. 1976, ApJ, 205, 419
Walborn, N. R. 1977, ApJ, 215, 53
Walborn, N. R. 1978, ApJ, 224, L133
Walborn, N. R. 1982, ApJ, 254, L15
Walborn, N. R. 1983, ApJ, 265, 716
Walborn, N. R., and Blades, J. C. 1986, ApJ, 304, L17
Walborn, N. R., and Fitzpatrick, E. L. 1990, PASP, 102, 379
Walborn, N. R., and Nichols-Bohlin, J. 1987, PASP, 99, 40
Walborn, N. R., Nichols-Bohlin, J., and Panek, R. J. 1985, International Ultraviolet Explorer Atlas of O-Type Spectra from 1200 to 1900 Å (NASA RP 1155)
Walborn, N. R., and Panek, R. J. 1984, ApJ, 280, L27
Walborn, N. R., and Panek, R. J. 1985, ApJ, 291, 806